 CMC, vol.6, no.3, pp.201-211, 2007

Numerical Simulation of Nonlinear Dynamic Responses of Beams Laminated with Giant Magnetostrictive Actuators

Haomiao Zhou[1,2], Youhe Zhou[1,3] and Xiaojing Zheng[1]

Abstract: This paper presents some simulation results of nonlinear dynamic responses for a laminated composite beam embedded by actuators of the giant magnetostrictive material (Terfenol-D) subjected to external magnetic fields, where the giant magnetostrictive materials utilizing the realignment of magnetic moments in response to applied magnetic fields generate nonlinear strains and forces significantly larger than those generated by other smart materials. To utilize the full potential application of the materials in the function and safety designs, e.g., active control of vibrations, the analysis of dynamic responses is requested in the designs as accurately as possible on the basis of those inherent nonlineary constitutive relations among stain, force and applied magnetic field existed in the materials. Here, a numerical code for the nonlinear vibration of laminated beams is proposed on the basis of a nonlinearly coupling constitutive model which fully behaves for the characteristics what are measured in experiments. It is found from this code that the natural frequency of the laminated beams changes with both the bias magnetic field and the pre-stresses, and the dynamic responses excited by an alternating magnetic field of simple harmonic form display strong nonlinear characteristics, for example, the frequency multiplication and the ultraharmonic resonance phenomena.

Keyword: Laminated beams, actuator layers of giant magnetostrictive material, analytical model of nonlinear constitutive model, nonlinear code of vibration analysis, frequency multiplication phenomenon, ultraharmonic resonance phenomenon

[1] Department of Mechanics and Engineering Science, College of Civil Engineering and Mechanics, Lanzhou University, Lanzhou 730000, P. R. China.
[2] College of Information Engineering, China Jiliang University, Hangzhou, 310018, P. R. China.
[3] Corresponding author. Tel: 086-0931-8910340; Fax: 086-0931-8625576; Email: zhouyh@lzu.edu.cn.

1 Introduction

With the development of aircraft and space engineering, the structures are requested to be as light as possible in weigh such that these structures are usually flexible, thereby some large amplitude vibrations are easily excited out [Iura and Atluri (1988)]. To suppress the undesired vibrations, some smart structures on the basis of active control of the operating structures associated with some smart materials, e.g., piezoelectric layers [Im and Atluri (1989), Cheng and Chen (2004), Wu, Lo and Chao (2005), Wu and Syu (2006), Han, Pan, Roy and Yue (2006), Zhou and Wang et al (2006), Dziatkiewicz and Fedelinski (2007)], shape memory alloys [Auricchio, Petrini, Pietrabissa and Sacco (2003)], and giant magnetostrictive materials [Zhou, Zheng and Zhou (2006), Zhou and Zhou (2007)], et al., either as sensors or actuators or both are designed in theory and engineering. Among these three materials, the first two materials have attracted the attention of many researchers in vibration control of flexible structures [Bailey and Hubbard (1985), Crawley and DeLuis (1987), Baz, Imam and Mccoy (1990), Zhou and Tzou (2000), Zhou and Wang (2004)]. At present, it is found that the giant magnetostrictive materials have some advantages over other smart materials when they are employed as actuators, for example, the smart materials have the ability to generate large strains and forces, the ability to fast act to external magnetic field, and the ability to retain their properties even in the particle form and easy embeddability into the host materials such as carbon fiber reinforce plastics (CFRP) and glass fiber reinforce plastics (GFRP)

[Marguet, Rozycki and Gornet (2006), Han, Ingber and Schreyer (2006)], as well as being attractive materials for high ratio of strength to weight [Subramanian (2002)].

Recently, the actuators of giant magnetostrictive materials were mainly employed in some expectant operating domain of the constitutive relations of the materials almost linearly changed with a magnetic bias field and a pre-stress [Anjanappa and Bi (1993), Krishna, Anjanappa and Wu (1997), Reddy and Barbosa (2000), Pradhan, Ng, Lam and Reedy (2001), Subramanian (2002), Kumar, Ganesan, Swarnamani and Padmanabhan (2003)]. The experimental measurements, however, indicate that these materials have strong nonlinearity among the stain, pre-stress and bias magnetic field [Moffett, Clark and Wun-Fogle (1991)], and the resonance frequency changes with the magnetic bias field for a Terfenol-D rod actuator [Savage, Clark and Powers (1975)]. The latter is due to the Young's modulus of a Terfenol-D rod changes nonlinearly with the stress and the magnetic field (the ΔE effect), and it is firstly simulated by Sun and Zheng [Sun and Zheng (2006)] after an analytical model of constitutive relations with close form to the smart materials was proposed by Zheng and Liu [Zheng and Liu (2005)], from which all characteristics measured in the experiments are fully behaved by the constitutive model (see Fig. 1). The other researches about theory and numerical simulation of dynamic response of Terfenol-D rod actuator can only simulated dynamic response under preset bias field and pre-stress[Engdahl and Svensson (1988), Tiberg, Bergqvist and Engdahl (1993), Freeman and Jr (1993), Jr and Freeman (1994), Koshi (1997), Davino, Natale, Pirozzi and Visone (2004)].

Here, we propose a numerical code to analyze the dynamic responses of beams laminated by some actuators of giant magnetostrictive material layers on the basis of the nonlinear constitutive model proposed by Zheng [Zheng and Liu (2005)]. In the following section, the theoretical model employed is introduced, while the numerical approach is presented in section 3. After the numerical results and discussions are displayed in section 4, some remarks are concluded in section

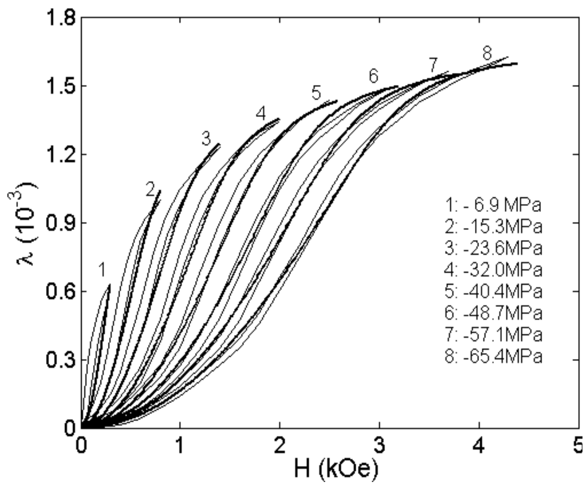

Figure 1: Experimental [Moffett, Clark and Wun-Fogle et al (1991)] and theoretical [Zheng and Liu (2005)] curves of magnetostrictive strain (hysteresis loops: experimental; solid lines: theoretical).

5.

2 Essential dynamic theory of the composite beam

Here, we consider a laminated composite beam with n layers in which $n-1$ layers are CFRP (Carbon Fiber Reinforced Plastic) plies and one layer is Terfenol-D particles (see Fig. 2). Without loss of generality, a cantilever beam fixed at $x=0$ and free at $x=L$ is dealt with in the following numerical code, and the Terfenol-D particles which are distributed on the above surface of the beam are set in a suitable resin, such as epoxy, and bonded to the neighboring CFRP layers, without any possibility of slip. In the present analysis, the weight of the resin is ignored. A series of closely packed magnetic coils, insulated from each other, enclosing the full beam is used to generate the bias and excited magnetic fields. Here, all CFRP layers are assumed to behave as a linear orthotropic medium, whereas the Terfenol-D layer behaves as an equivalent isotropic medium. The fiber orientations in CFRP layers are distributed arbitraryly. It is assumed that the cross-section of the beam being uniform about the y-axis and the deformations in the $x-y$ plane are infinitesimally small, since the beam has very high flexural stiffness in the $x-y$ plane compared to the $x-z$ plane.

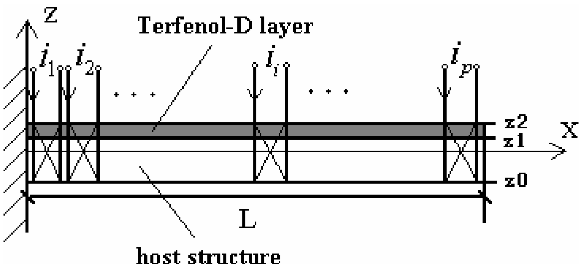

Figure 2: A typical laminate composite beam with an embedded magnetostrictive layer.

For the deflection of the composite beam in transverse or z-direction, the hypothesis of the Bernoulli-Euler theory of the beam is employed. Denote the in-plane extension displacement by $u_0(x,t)$ in the middle-plane and the deflection function by $w(x,t)$ at $z=0$. Then, the displacement field can be written as

$$\begin{aligned} &u(x,y,z,t) = u_0(x,t) - z\frac{dw}{dx}, \\ &v(x,y,z,t) \equiv 0, \\ &w(x,y,z,t) = w(x,t) \end{aligned} \tag{1}$$

Further, the strain along x-axis is formulated by

$$\varepsilon = \varepsilon^0 - z\kappa = \frac{du_0}{dx} - z\frac{d^2w}{dx^2} \tag{2}$$

For the CFRP layers, the constitutive relation is of the form

$$\sigma^{(i)} = \overline{Q}_{11}^{(i)}\varepsilon^{(i)} \tag{3}$$

where the superscript i represents the layer number and

$$\begin{aligned} \overline{Q}_{11}^{(i)} =& Q_{11}^{(i)}\cos^4\theta^{(i)} + 2\left(Q_{12}^{(i)} + 2Q_{66}^{(i)}\right) \\ & \cdot\cos^2\theta^{(i)}\sin^2\theta^{(i)} + Q_{22}^{(i)}\sin^4\theta^{(i)} \\ Q_{11}^{(i)} =& E_{11}^{(i)} \Big/ \left(1 - \nu_{12}^{(i)}\nu_{21}^{(i)}\right), \\ Q_{22}^{(i)} =& E_{22}^{(i)} \Big/ \left(1 - \nu_{12}^{(i)}\nu_{21}^{(i)}\right) \\ Q_{21}^{(i)} =& Q_{12}^{(i)} = \nu_{21}^{(i)}E_{11}^{(i)} \Big/ \left(1 - \nu_{12}^{(i)}\nu_{21}^{(i)}\right), \\ Q_{66}^{(i)} =& G_{12}^{(i)} \end{aligned} \tag{4}$$

For the giant magnetostrictive material, e.g., Terfenol-D particles layer, the input current of coil generates a magnetic field to drive the beam deformation, which yields an output response of nonlinear displacement varying with the magnetic field. To this case, the analytical equations of nonlinear constitutive relations of giant magnetostrictive material proposed by Zheng [Zheng and Liu (2005)] are here employed, i.e.,

$$\varepsilon = \frac{\sigma}{E_s} + \begin{cases} \lambda_s \tanh\frac{\sigma}{\sigma_s} + \left[1 - \tanh\frac{\sigma}{\sigma_s}\right]\frac{\lambda_s}{M_s^2}M^2 & \frac{\sigma}{\sigma_s} \geq 0 \\ \frac{\lambda_s}{2}\tanh\frac{2\sigma}{\sigma_s} + \left[1 - \frac{1}{2}\tanh\frac{2\sigma}{\sigma_s}\right]\frac{\lambda_s}{M_s^2}M^2 & \frac{\sigma}{\sigma_s} < 0 \end{cases} \tag{5}$$

$$H = \frac{1}{k}f^{-1}\frac{M}{M_s} - \begin{cases} 2\left\{\sigma - \sigma_s \ln\left[\cosh\frac{\sigma}{\sigma_s}\right]\right\}\frac{\lambda_s}{\mu_0 M_s^2}M & \frac{\sigma}{\sigma_s} \geq 0 \\ 2\left\{\sigma - \frac{\sigma_s}{4}\ln\left[\cosh\frac{2\sigma}{\sigma_s}\right]\right\}\frac{\lambda_s}{\mu_0 M_s^2}M & \frac{\sigma}{\sigma_s} < 0 \end{cases} \tag{6}$$

where $f(x) = \coth(x) - 1/x$, the relaxation factor $k = 3\chi_m/M_s$, χ_m is linear magnetic susceptibility, E_s is the saturation Young's modulus and E_0 is initial Young's modulus, $\sigma_s = \lambda_s E_s E_0/(E_s - E_0)$, λ_s is the saturation magnetostrictive coefficient,M_s is the saturation magnetization and $\mu_0 = 4\pi \times 10^{-7}$H/m is the vacuum permeability.

According to Eq.(5), one sees that the first term in the right hand of it is independent with magnetic field, and the last two terms is nonlinearly relevant to the magnetostrictive stain, denoted by $\lambda(\sigma,H)$, induced by magnetic field. So the nonlinear constitutive equations can be re-written as

$$\varepsilon = \frac{\sigma}{E(\sigma)} + \lambda(\sigma,H) \tag{7}$$

According to Eqs. (3) and (7), The constitutive relation of all layers can be uniformly written as the form

$$\sigma = Q\varepsilon - Q\lambda(\sigma,H) \tag{8}$$

where $Q\lambda(\sigma,H)$ is the equivalent stress induced by Terfenol-D layer. Here, $Q = E(\sigma)$ when the layer is made of the Terfenol-D materials, and

$Q=\overline{Q}_{11}^{(i)}$ and $Q\lambda(\sigma,H)=0$ in CFRP ones. Substitution Eq. (2) into Eq. (8) and integrating the resulting equation along z-direction, we get the matrix form of the constitutive relations as fellows

$$\begin{Bmatrix} N \\ M \end{Bmatrix} = \begin{bmatrix} A & C \\ C & D \end{bmatrix} \begin{Bmatrix} \varepsilon^0 \\ \kappa \end{Bmatrix} - \begin{Bmatrix} N_\Lambda \\ M_\Lambda \end{Bmatrix} \tag{9}$$

in which $A=\int_{-h/2}^{h/2} Qdz$, $B=\int_{-h/2}^{h/2} Qzdz$, $D=\int_{-h/2}^{h/2} Qz^2dz$, $N=\int_h \{\sigma\}dz$, $M=\int_h \{\sigma\}zdz$, $N_\Lambda=\int_{h_a} Q\lambda(\sigma,H)dz$ and $M_\Lambda=\int_{h_a} zQ\lambda(\sigma,H)dz$. Here, the thickness of the beam and the Terfenol-D layer are respectively h and h_a. From the physical meaning, we know that N and M are the internal force and moment, respectively; while N_Λ and M_Λ are their parts contributed by the Terfenol-D layer.

After that, the strain energy of laminate beam under an applied magnetic field can be expressed by the form

$$U=\frac{1}{2}\iint\limits_S \begin{Bmatrix} \varepsilon^{0T} & \kappa^T \end{Bmatrix} \begin{bmatrix} A & C \\ C & D \end{bmatrix} \begin{Bmatrix} \varepsilon^0 \\ \kappa \end{Bmatrix} dA - \iint\limits_S \int_0^{\{\varepsilon^0,k\}^T} \begin{Bmatrix} N_\Lambda \\ M_\Lambda \end{Bmatrix}^T \begin{Bmatrix} d\varepsilon^0 \\ d\kappa \end{Bmatrix} dA \tag{10}$$

where S stands for the area of cross-section of the beam. Denote $\{r\}=[u_0 \; w]^T$. We have

$$\begin{Bmatrix} \varepsilon^0 \\ \kappa \end{Bmatrix} = \begin{bmatrix} \frac{\partial}{\partial x} & 0 \\ 0 & -\frac{\partial^2}{\partial x^2} \end{bmatrix} \begin{Bmatrix} u_0 \\ w \end{Bmatrix} = [L]\{r\} \tag{11}$$

Then, the displacement vector at any point of the laminate beam can be written as,

$$\begin{Bmatrix} X \\ Z \end{Bmatrix} = \begin{bmatrix} 1 & -z\frac{\partial}{\partial x} \\ 0 & 1 \end{bmatrix} \begin{Bmatrix} u_0 \\ w \end{Bmatrix} = [\Psi]\{r\} \tag{12}$$

Thus, the kinetic energy and the work of external forces of laminate beam can be respectively formulated as the matrix forms, i.e.,

$$\begin{aligned} T &= \iiint\limits_V \frac{1}{2}\rho \begin{Bmatrix} \dot{X} & \dot{Z} \end{Bmatrix} \begin{Bmatrix} \dot{X} \\ \dot{Z} \end{Bmatrix} dV \\ &= \iiint\limits_V \frac{1}{2}\rho \dot{r}^T [\Psi]^T [\Psi] \dot{r} dV \end{aligned} \tag{13}$$

$$W=\iint\limits_A r^T f dA + \int\limits_l r^T \overline{f} dl + \sum_{i=1}^N F_i r_i \tag{14}$$

Here, f indicates the plane distributed force or moment, $\overline{f}$ is the line distributed force or moment, and F denotes the concentrated force or moment.

Dividing the beam with n beam elements with two nodes along longitudinal direction, and every node with three freedom (u_0,w,α), where $\alpha=dw/dx$. Denote $\delta_i=[u_i \; w_i \; \alpha_i]$ $(i=1,2)$, and $\{\delta^e\}=[\delta_1 \; \delta_2]^T$. Then applying the Lagrangian interpolation polynomial to the displacement function, we get the displacement in each element that may be expressed in the terms of the node displacement column, i.e.,

$$\{r\}=\begin{bmatrix} N_1 & N_2 \end{bmatrix} \begin{Bmatrix} \delta_1^T \\ \delta_2^T \end{Bmatrix} = [N]\{\delta^e\} \tag{15}$$

Substituting Eq. (15) into Eq. (11), one obtains

$$\begin{Bmatrix} \varepsilon^0 \\ \kappa \end{Bmatrix} = [L]\{r\} = [L][N]\{\delta^e\} = [B]\{\delta^e\} \tag{16}$$

Substituting Eqs. (15), (16) into Eqs. (10), (13) and (14), then we get the element energy functional in the form,

$$\begin{aligned} \Pi =& (T-U+W) \\ =& \frac{1}{2}\iint\limits_A \Bigg(\dot{\delta}^{eT} \left(\int_t (\Psi N)^T \rho \Psi N dz \right) \dot{\delta}^e \\ & - \delta^{eT} B^T \begin{bmatrix} A & C \\ C & D \end{bmatrix} B\delta^e + 2\delta^{eT} B^T \begin{bmatrix} N_\Lambda \\ M_\Lambda \end{bmatrix} \\ & + 2\delta^{eT} N^T f \Bigg) dA + \int_l \delta^{eT} N^T \overline{f} dl \end{aligned} \tag{17}$$

Applied the Halmiltonian principle $\delta\int_{t_1}^{t_2}\Pi dt=0$, we obtain a system of ordinary differential Equations of the dynamic system in the matrix form,

$$[\mathbf{M}]\{\ddot{\mathbf{a}}\}+[\mathbf{C}]\{\dot{\mathbf{a}}\}+[\mathbf{K}(\sigma)]\{\mathbf{a}\}=\{\mathbf{F}(H,\sigma)\} \tag{18}$$

Here, $\ddot{\mathbf{a}}$ and $\mathbf{a}$ are respectively the columns of node acceleration and displacement, $\mathbf{M}$, $\mathbf{K}$, $\mathbf{C}$ and $\mathbf{F}$ are respectively the mass matrix, the stiffness matrix, the damping matrix (looked as linear combination of **M** and **K**) and the load column. They are explicitly formulated by

$$[\mathbf{M}] = \sum_e \iint_{S_e} \left(\int_h (\Psi N)^T \rho \Psi N dz \right) dA \tag{19}$$

$$[\mathbf{K}] = \sum_e \iint_{S_e} B^T \begin{bmatrix} A & C \\ C & D \end{bmatrix} B dA \tag{20}$$

$$\{\mathbf{F}\} = \{\mathbf{F}_a\} + \{\mathbf{F}_f\} + \left\{\mathbf{F}_{\overline{f}}\right\} \tag{21}$$

$$\begin{aligned} \mathbf{F}_a &= \sum_e \iint_{S_e} B^T \begin{bmatrix} N_\Lambda \\ M_\Lambda \end{bmatrix} dA, \\ \mathbf{F}_f &= \sum_e \iint_{S_e} N^T f dA, \\ \mathbf{F}_{\overline{f}} &= \sum_e \int_{l_e} N^T \overline{f} dA \end{aligned} \tag{22}$$

It is noted that the stiffness matrix $\mathbf{K}(\sigma)$ and the load column $\mathbf{F}(H,\sigma)$ are nonlinearly relative to stress in the beam at instant, so Eq. (18) is a set of nonlinear dynamic equations.

3 Numerical approach

In order to solve the nonlinear ordinary differential equations of Eq. (18), the Newmark method is here employed. After that, Eq. (18) is converted into the following difference equation

$$M\ddot{a}_{t+\Delta t} + C\dot{a}_{t+\Delta t} + K a_{t+\Delta t} = F_{t+\Delta t} \tag{23}$$

where

$$\dot{a}_{t+\Delta t} = \dot{a}_t + [(1-\beta)\ddot{a}_t + \beta \ddot{a}_{t+\Delta t}]\Delta t \tag{24}$$

$$a_{t+\Delta t} = a_t + \dot{a}_t \Delta t + \left[\left(\frac{1}{2} - \alpha \right) \ddot{a}_t + \alpha \ddot{a}_{t+\Delta t} \right] \Delta t^2 \tag{25}$$

Here, Δt indicates the time step, α and β are the parameters of the Newmark method. According to Eq. (25), we obtain

$$\ddot{a}_{t+\Delta t} = \frac{1}{\alpha \Delta t^2}(a_{t+\Delta t} - a_t) - \frac{1}{\alpha \Delta t}\dot{a}_t - \left(\frac{1}{2\alpha} - 1 \right) \ddot{a}_t \tag{26}$$

Substituting equation (26) into equation (24) then the result equation and equation (26) into equation (23), we get the system of algebraic equations at time step $t + \Delta t$ of the form

$$\begin{aligned} &\left(K + \frac{1}{\alpha \Delta t^2} M + \frac{\delta}{\alpha \Delta t} C \right) a_{t+\Delta t} \\ &= F_{t+\Delta t} + M \left[\frac{1}{\alpha \Delta t^2} a_t + \frac{1}{\alpha \Delta t} \dot{a}_t + \left(\frac{1}{2\alpha} - 1 \right) \ddot{a}_t \right] \\ &+ C \left[\frac{\delta}{\alpha \Delta t} a_t + \left(\frac{\delta}{\alpha} - 1 \right) \dot{a}_t + \left(\frac{\delta}{2\alpha} - 1 \right) \Delta t \ddot{a}_t \right] \end{aligned} \tag{27}$$

Once the quantities of $\mathbf{a}_t$, $\dot{\mathbf{a}}_t$, and $\ddot{\mathbf{a}}_t$ at time step t are known, it is obvious that $\mathbf{a}_{t+\Delta t}$ can be gained by the above equation. Then $\ddot{\mathbf{a}}_{t+\Delta t}$ and $\dot{\mathbf{a}}_{t+\Delta t}$ are determined by equations (26) and (24), respectively. In the following calculations, the parameters in the Newmark method are taken as $\beta = 0.5$ and $\alpha = 0.25(0.5+\beta)^2$.

Due to the nonlinear coupling as shown in the previous section, equation (27) is nonlinear on the unknowns at each time step, which is relative to $E(\sigma)$ and $\lambda(\sigma, H)$, when a bias magnetic field H_{bias} and a pre-stress σ_0 are specified. In order to solve this nonlinear coupling, here, an iteration approach is employed. The main steps of the approach are briefly introduced as follows:

Step 1 At the initial moment t_0, the displacement a_0, velocity $\dot{a}_0$, acceleration $\ddot{a}_0$ and the initial stress σ_{0i} should be given.

Step 2 The mass matrix M, the damping matrix C and the stiffness matrix K can be integrated based on Eqs. (19)-(21), and there is $\sigma_x = \sigma_{0i}$ in the stiffness matrix K at the moment. The time step is chosen as $\Delta t = 2.5 \times 10^{-4}$. A series of constants such as $c_0 = \frac{1}{\alpha \Delta t^2}$, $c_1 = \frac{\delta}{\alpha \Delta t}$, $c_2 = \frac{1}{\alpha \Delta t}$, $c_3 = \frac{1}{2\alpha} - 1$, $c_4 = \frac{\delta}{\alpha} - 1$, $c_5 = \frac{\Delta t}{2}\left(\frac{\delta}{\alpha} - 2\right)$, $c_6 = \Delta t(1-\delta)$, $c_7 = \delta \Delta t$ are calculated.

Step 3 After the effective stiffness matrix $\hat{K} = K + c_0 M + c_1 C$ is gained, the load column $F_{t+\Delta t}$ at the moment $t + \Delta t$ can be integrated based on Eq. (22), i.e., $\hat{F}_{t+\Delta t} = F_{t+\Delta t} + M(c_0 a_t + c_2 \dot{a}_t + c_3 \ddot{a}_t) + C(c_1 a_t + c_4 \dot{a}_t + c_5 \ddot{a}_t)$ is obtained, and there are $\sigma_x = \sigma_{0i}$ and $H = H_{t+\Delta t}$ in the load array $F_{t+\Delta t}$ at the moment.

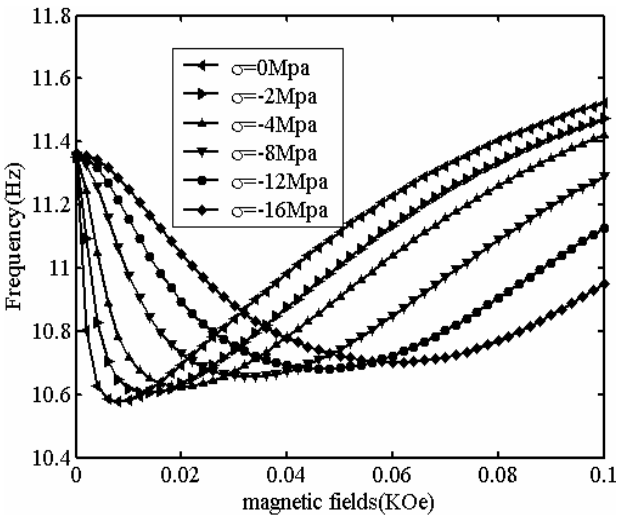

Figure 3: The curves of resonance frequency with magnetic bias field.

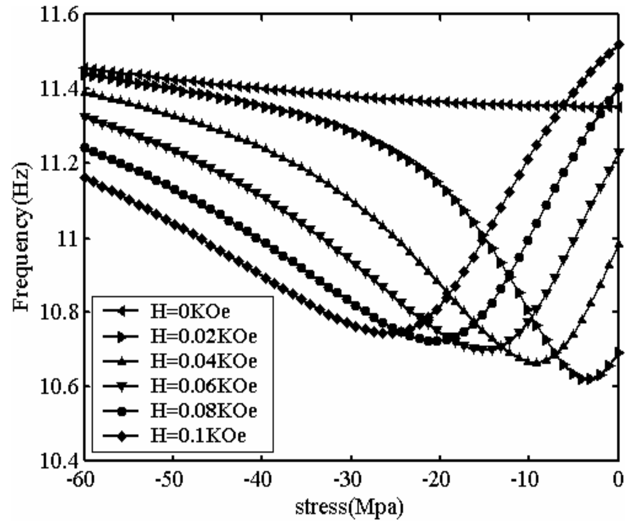

Figure 4: The curves of resonance frequency with compression pre-stress.

Step 4 The displacement $a_{t+\Delta t}$ at the moment $t+\Delta t$ is solved based on $\hat{K}a_{t+\Delta t} = \hat{F}_{t+\Delta t}$, then the acceleration$\ddot{a}_{t+\Delta t}$ and the velocity$\dot{a}_{t+\Delta t}$are gained respectively based on the expressions $\ddot{a}_{t+\Delta t} = c_0(a_{t+\Delta t} - a_t) - c_2\dot{a}_t - c_3\ddot{a}_t$ and $\dot{a}_{t+\Delta t} = \dot{a}_t + c_6\ddot{a}_t + c_7\ddot{a}_{t+\Delta t}$. The iteration process should be used in calculating the stiffness matrix K and the load array $F_{t+\Delta t}$ for the stress σ_x. The strain $\varepsilon_{t+\Delta t}$ at the moment $t+\Delta t$ is got based on equation (2) when u is replaced by $a_{t+\Delta t}$, thus a modified stress $\sigma_{0(i+1)} = E_i(\sigma_{0i})\varepsilon_{0(i+1)}$ at the moment is got based on the expression $\varepsilon_{0(i+1)} = \varepsilon_{t+\Delta t} - \lambda(\sigma_{0i}, H_{t+\Delta t})$. If $\sigma_{0(i+1)}$ does not satisfy precision $\|\Delta\sigma_0\| < \delta$ ($\delta = 1\times10^{-5}$), replacing σ_{0i} by $\sigma_{0(i+1)}$ and going to step 2) until it satisfies the precision condition, otherwise $\sigma_{0(i+1)}$ is the true stress of the rod at the moment. Replacing σ_{0i} by $\sigma_{0(i+1)}$, t by $t+\Delta t$ and going to step 2), the next step is going on.

Repeating the steps (2)-(4), the deflection of the beam at any moment t are reached.

4 Numerical Results and Discussion

Here, we give a case study of a laminated beam which has the length of 1m, the width of 10mm, and considered beam have ten layers of 1mm thickness each. The magnetostrictive layer is located in above surface of the laminated beam, and the fiber angle with respect to the x-axis in the x-y plane is zero degree in the other CFRP layers. The material properties of the CFRP layers are $E_{11} = 138.6$GPa, $E_{22} = 138.6$GPa, $G_{12} = 138.6$GPa, $v_{12} = v_{21} = 0.26$ and $\rho = 1824$kg/m^3. The properties of the Terfenol-D layer are respectively taken as $\rho = 9250kg/m^3$, $\lambda_s = 1300$ppm, $\mu_0 M_s = 0.8$T, $E_s = 110$Gpa, $\sigma_s = 200$Mpa and $\chi_m = 80$ when $\sigma = 0$. External magnetic field in constitutive equation (8) are composed of magnetic bias field H_{bias} and simple harmonic magnetic fields $H_0\sin(2\pi\omega t)$, so the total magnetic field is expressed as $H(t) = H_{bias} + H_0\sin(2\pi\omega t)$.

First of all, we give the vibration characteristic of the beam structure without application of magnetic field and pre-stress. The numerical resuts display that the first five natural frequency of laminated beam at the initial moment are $f_1 = 11.35$Hz, $f_2 = 71.15$Hz, $f_3 = 199.26$Hz, $f_4 = 390.696$Hz and $f_5 = 646.74$Hz respectively. In fact, the natural frequency change nonlinearly with the stress and the magnetic field, it is due to ΔE effect. Fig. 3 is the curves of first-order resonance frequency changing with the magnetic field for given pre-stresses. It can be seen that

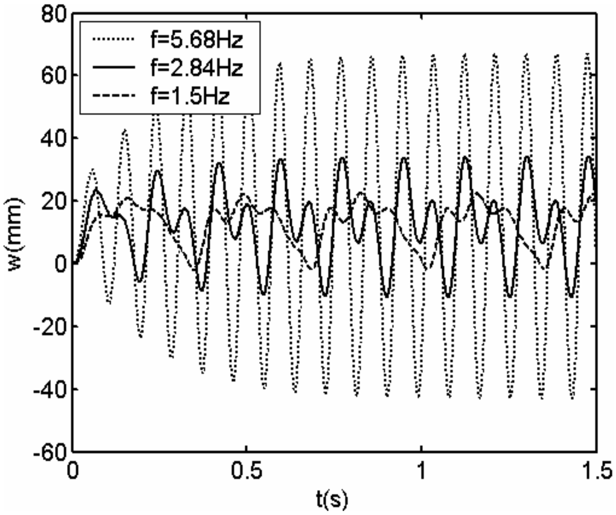

Figure 5: The response curves of amplitude of the free end of the beam when $H_{bias} \equiv 0$, $\sigma_0 = 0$Mpa and the amplitude of excited magnetic field $H_0 = 0.1$KOe.

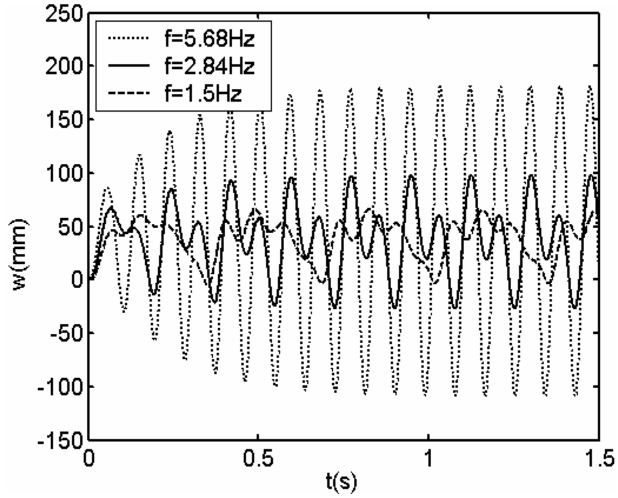

Figure 6: The response curves of amplitude of the free end of the beam when $H_{bias} \equiv 0$, $\sigma_0 = 0$Mpa and the amplitude of excited magnetic field $H_0 = 0.4$KOe.

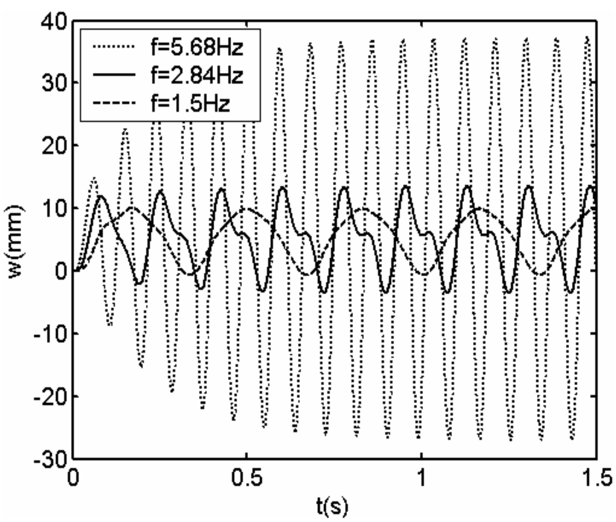

Figure 7: The response curves of amplitude of the free end of the beam when $H_{bias} \equiv 0$, $\sigma_0 = -6.94$Mpa and the amplitude of excited magnetic field $H_0 = 0.1$KOe.

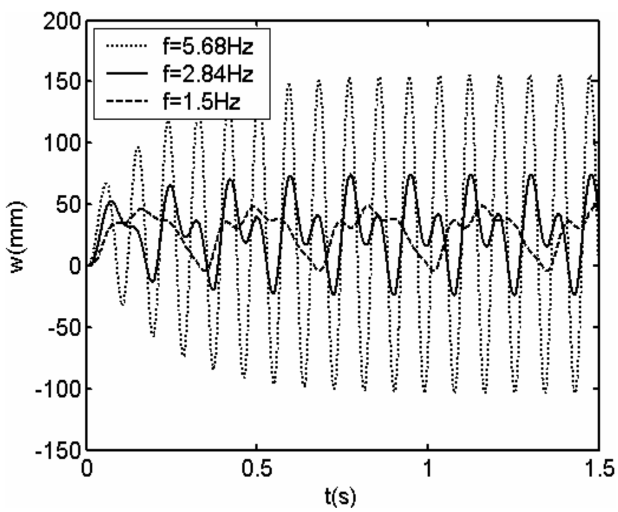

Figure 8: The response curves of amplitude of the free end of the beam when $H_{bias} \equiv 0$, $\sigma_0 = -6.94$Mpa and the amplitude of excited magnetic field $H_0 = 0.4$KOe.

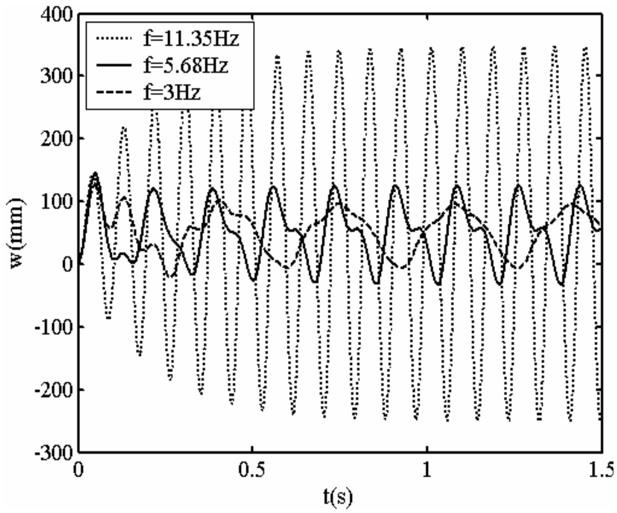

Figure 9: The response curves of amplitude of the free end of the beam when $H_{bias} = 0.4$KOe, $\sigma_0 = 0$Mpa and the amplitude of excited magnetic field $H_0 = 0.4$KOe.

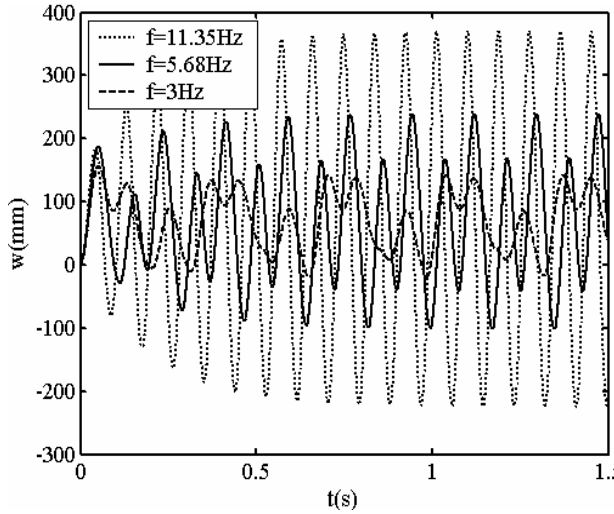

Figure 10: The response curves of amplitude of the free end of the beam when $H_{bias} = 0.4$KOe, $\sigma_0 = 0$Mpa and the amplitude of excited magnetic field $H_0 = 0.8$KOe.

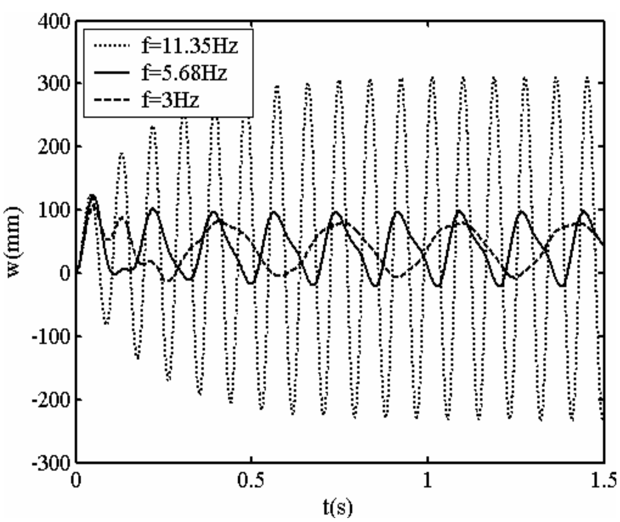

Figure 11: The response curves of amplitude of the free end of the beam when $H_{bias} = 0.4$KOe, $\sigma_0 = -6.94$Mpa and the amplitude of excited magnetic field $H_0 = 0.4$KOe.

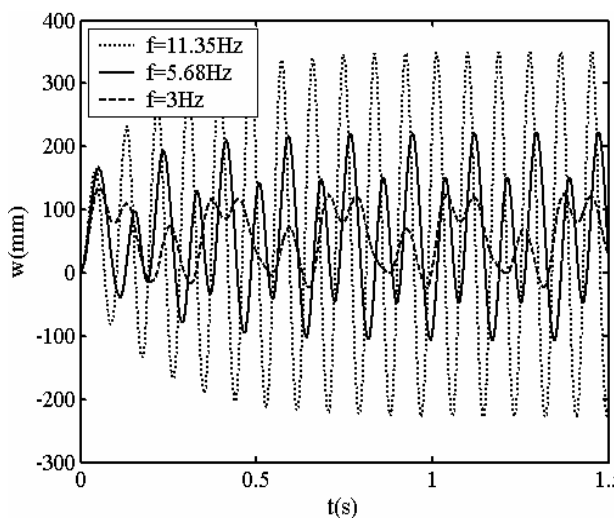

Figure 12: The response curves of amplitude of the free end of the beam when $H_{bias} = 0.4$KOe, $\sigma_0 = -6.94$Mpa and the amplitude of excited magnetic field $H_0 = 0.8$KOe.

the resonance frequency decreases up to a critical value rapidly and then slightly increases with the further increase of magnetic field, and the critical magnetic field will increase with the increase of compressive pre-stress. Fig. 4 is the curves of resonance frequency change with the compressive pre-stress for given magnetic field. It can be seen that the resonance frequency decreases up to a critical value slightly and then rapidly increases with the further increase of pre-stress except the curve of $H = 0$KOe. Then we can calculate the dynamic response of beam under external magnetic field with variant frequency and amplitude. In Figs. 5-8 are shown the results of displacement response of the free end of the composite beam when $H_{bias} \equiv 0$, and the frequency of external magnetic field are $\omega = 5.68$Hz, $\omega = 2.84$ Hz and $\omega = 1.50$Hz respectively. Here, Figs. 5-6 are the response results when pre-stress $\sigma_0 = 0$Mpa and the amplitude of external magnetic field are respectively $H_0 = 0.1$KOe and $H_0 = 0.4$KOe. And Figs. 7-8 are the response results when $\sigma_0 = -6.94$Mpa and the amplitude of external magnetic field are respectively $H_0 = 0.1$KOe and $H_0 = 0.4$KOe. It can be seen from Fig. 5 that the fundamental natural vibration will appear when the frequency of external magnetic field $\omega = 5.68$Hz (the frequency of external magnetic field is equal to half of first-order natural frequency of beam), that is, the frequency multiplication phenomena. We can see also that the ultraharmonic resonance phenomena when the frequency of external magnetic field $\omega = 2.84$Hz (the frequency of external magnetic field is equal to quarter of first-order natural frequency of beam). The results of Fig. 6, the amplitude of external magnetic field is 0.4KOe, are similar with Fig. 5. The amplitude of displacement response in Fig. 6 is larger than the result in Fig. 5, but this augmentation of amplitude is nonlinear with the augmentation of magnetic field. Figs 7-8 have applied pre-stress $\sigma_0 = -6.94$Mpa compared with Figs. 5-6. It can be seen from comparison of those figures that amplitude of vibration will decreased and the ultraharmonic resonance phenomena will weaken in low field because of pre-stress (see Fig. 5 and Fig. 7, or see Fig. 6 and Fig. 8).

Frequency multiplication and ultraharmonic resonance phenomena will almost vanish if applied bias field in the Terfenol-D layer of beam, that is, it correspond linear piezomagnetic model. Figs. 9-12 showed the dynamic response of free end of laminated beam when bias magnetic field $H_{bias} = 0.4$KOe, the amplitude of external magnetic field are respectively $H_0 = 0.4$KOe and $H_0 = 0.8$KOe, the frequency of external magnetic field are $\omega = 11.35$Hz, $\omega = 5.68$Hz and $\omega = 3$Hz. Here, Figs. 9-10 are the response results when pre-stress $\sigma_0 = 0$Mpa and the amplitude of external magnetic field are respectively $H_0 = 0.4$KOe and $H_0 = 0.8$KOe. And Figs. 11-12 are the response results when $\sigma_0 = -6.94$Mpa and the amplitude of external magnetic field are respectively $H_0 = 0.4$KOe and $H_0 = 0.8$KOe. It can be seen from Fig. 9 that the fundamental natural vibration will appear when the frequency of external magnetic field $\omega = 11.35$Hz (the frequency of external magnetic field is equal to first-order natural frequency of beam), and also the response frequency will equal to frequency of external magnetic field when $\omega = 5.68$Hz and $\omega = 3$Hz. That is, The dynamic response of Fig. 9 is linear. Compared with Fig. 9 we can see from Fig. 10 more visible high-order harmonic component because of excite field $H_0 = 0.8$KOe larger than bias field $H_{bias} = 0.4$KOe in Fig. 10. Figs 11-12 have pre-stress $\sigma_0 = -6.94$Mpa compared with Figs. 9-10. It can be seen from comparison of those figures (see Fig. 9 and Fig. 11, or see Fig. 10 and Fig. 12) that amplitude of vibration will decrease, response curve will more smooth and more similar with linear vibration because of applied pre-stress (show in Fig. 11).

5 Conclusions

Based on a new nonlinear constitutive relation, a nonlinear dynamic model of composite beam with one magnetostrictive layer actuator is presented. This dynamic model can predicted the resonance frequency change with bias magnetic field and pre-stress. Moreover the simulation results of dynamic response show obvious nonlinear characteristics, such as the frequency multiplication and the ultraharmonic resonance phenomena, when have not applied bias field. So, it is necessary for us to consider the nonlinear characteristics of magnetostrictive materials and dynamic response in industrial application, such as sensor and actuator in vibration active control, and this research will provide theory base for application.

Acknowledgement: This research was supported by a grant of the Fund of the National Natural Science Fund of China for Outstanding Young Researchers (No. 10025208), the Fund of Pre-Research for Key Basic Researches of the Ministry of Science and Technology of China, the Fund of Natural Science Foundation of China (No. 90405005), the Fund of Ministry of Education of China for the Original Research Team in New Century, and the Science Fund of the Ministry of Education of China for Ph.D. Program. The authors gratefully acknowledge these supports. The authors sincerely appreciate these supports to this research.

References

Anjanappa, M.; Bi, J. (1993): Modelling, design and control of embedded Terfenol-D actuator. *Proc. SPIE-Smart Structures and Intelligent Systems*, 1917, 908-918.

Auricchio, F.; Petrini, L.; Pietrabissa, R.; Sacco, E. (2003): Numerical modeling of shape-memory alloys in orthodontics. *CMES: Computer Modeling In Engineering & Sciences*, 4(3&4), 365-380.

Bailey, T.; Hubbard, J. E. (1985): Distributed piezoelectric polymer active vibration control of a cantilever beam. *Journal of Guidance, control and Dynamics,* 8, 1199-1206.

Baz, A.; Imam, K.; Mccoy, J. (1990): Active vibration control of flexible beams using shape memory actuators. *J. Sound Vib*, 140, 437-456.

Cheng, C. H.; Chen, S. C. (2004): The simulation of diaphragm deflection actuated by shear mode piezoelectric actuator in microdroplet ejector. *CMC: Computers Materials & Continua*, 1(3), 205-212.

Crawley, E. F.; DeLuis, J. (1987): Use of piezoelectric actuators as elements of intelligent structures. *American Institute of Aeronautics and Astronautics Journal*, 25(10), 1373-1385.

Davino, D.; Natale, C.; Pirozzi, S.; Visone, C. (2004): Phenomenological dynamic model of a magnetostrictive actuator. *Physica B*, 343, 112-116.

Dziatkiewicz, G.; Fedelinski, P. (2007) Dynamic analysis of piezoelectric structures by the dual reciprocity boundary element method. *CMES: Computer Modeling in Engineering & Sciences*, 17(1), 35-46.

Engdahl, G.; Svensson, L. (1988): Simulation of the magnetostrictive performance of Terfenol-D in mechanical devices. *J. Appl. Phys*, 63(8), 3924-3926.

Freeman, M. R.; Nunes, Jr, G. (1993): Studies of dynamic magnetostriction by time-resolved scanning fiber interferometry. *Appl. Phys. Lett.*, 63(9), 1200-1202.

Han, F.; Pan, E.; Roy, A. K.; Yue, Z. Q. (2006), Responses of piezoelectric, transversely isotropic, functionally graded, and multilayered half spaces to uniform circular surface loadings. *CMC: Computers Materials & Continua*, 14(1),15-29.

Han, R.; Ingber, M. S.; Schreyer, H. L. (2006) Progression of failure in fiber-reinforced materials. *CMC: Computers Materials & Continua*, 4(3), 163-176.

Im, S.; Atluri, S. N. (1989): Effects of a Piezo-Actuator on a Finitely Deformed Beam Subjected to General Loading. *AIAA Journal*, 27(12), 1801-1807.

Iura, M.; Atluri, S. N. (1988): Nonlinearities in Dynamics & Control of Space Structures:-Some Issues for Computational Mechanics. *Large Space Structures:-Dynamics and control*, Atluri, S. N.; Amos, A. K. Eds., Springer-Verlag, Berlin, Chapter 3.

Jr, G. N.; Freeman, M. R. (1994): Time-resolved scanning probe microscopy: Investigations and applications of dynamic magnetostriction (invited). *J.Appl.Phys.*, 75(10), 6205-6210.

Koshi, K. (1997): Dynamic behaviour of Terfenol-D. *Journal of Alloys and compounds*, 258, 56-60.

Krishna, M. A. V.; Anjanappa, M.; and Wu, Y. F. (1997): The use of magnetostrictive particle actuators for vibration attenuation of flexible beams. *J. Sound Vib*, 206, 133-49.

Kumar, J. S.; Ganesan, N.; Swarnamani, S.; Padmanabhan, C. (2003): Active control of beam with magnetostrictive layer. *Computer and structure*, 81, 1375-1382.

Marguet, S.; Rozycki, P.; Gornet, L. (2006): A rate dependent constitutive model for glass-fibre/epoxy-matrix woven fabrics. *CMC: Computers Materials & Continua*, 4(3), 119-135.

Moffett, M. B.; Clark, A. E.; Wun-Fogle, M. (1991): Charaterization of Terfenol-D for magnetostrictive transducers. *J. Acoust. Soc. Am*, 89(3), 1448-1455.

Pradhan, S. C.; Ng, T. Y.; Lam, K. Y.; Reedy, J. N. (2001): Control of laminated composite plates using magnetostrictive layers. *Smart Mater. Struct.*, 10, 657-667.

Reddy, J. N.; Barbosa, J. I. (2000): On vibration suppression of magnetostrictive beams. *Smart Mater. Struct.* 9, 49-58.

Savage, H. T.; Clark, A. E.; Powers, J. H. (1975): Magnetomechanical coupling and E effect in highly magnetostrictive rare earth-Fe_2 compounds. *IEEE Transactions on Magnetics*, 11(5), 1355-1357.

Subramanian, P. (2002): Vibration suppression of symmetric laminated composite beams. *Smart Mater. Struct.*, 11, 880-885.

Sun, L.; Zheng, X. J. (2006) Numerical simulation on coupling behavior of Terfenol-D rods. *International Journal of solids and structures*, 43(6), 1613-1623.

Tiberg, H.; Bergqvist, A.; Engdahl, G. (1993): Evaluation of a magnetostrictive drive element model. *J. Appl. Phys*, 73(10), 5851-5853

Wu, C. P.; Lo, J. Y.; Chao, J. K. (2005): A three-dimensional asymptotic theory of laminated piezoelectric shells. *CMC: Computers Materials & Continua*, 2(2),119-137.

Wu, C. P.; Syu, Y. S. (2006): Asymptotic solutions for multilayered piezoelectric cylinders under electromechanical loads. *CMC: Computers Materials & Continua*, 4(2), 87-107.

Zheng, X. J.; Liu, X. E. (2005): A Nonlinear Constitutive Model for Terfenol-D Rods. *J. Appl. Phys*, 97, 053901.

Zhou, H. M.; Wang, J.; Zhou, Y. H.; Zheng, X. J. (2006): Optimal Track Seeking Control of Dual-Stage Actuator for High Density Hard Disk Drives. *ACTA Mechanica Solida Sinica*, 19(4), 297-306.

Zhou, H. M.; Zheng, X. j.; Zhou, Y. H. (2006): Vibration active control of nonlinear giant magnetostrictive actuators. *Smart materials and structure*, 15, 792-798.

Zhou, H. M.; Zhou, Y. H. (2007): Vibration Suppression Of Laminated Composite Beams Using Actuators Of Giant Magnetostrictive Materials. *Smart Materials and Structure*, 16,198-206.

Zhou, Y. H.; Wang, J. Z. (2004): Vibration control of piezoelectric beam-type plates with geometrical nonlinear deformation. *International Journal of Non-Linear Mechanics*, 39, 909-920.

Zhou, Y. H.; Tzou, H. S. (2000): Active control of nonlinear piezoelectric circular spherical shells. *International Journal of Solids and Structures*, 37, 1663-1677.